Transient temperature asymmetry between hemispheres in the Paleogene Atlantic Ocean

Zhonghui Liu[1, 2*], Yuxin He[3], Yiqing Jiang[1], Huanye Wang[2], Weiguo Liu[2], Steven M. Bohaty[4], Paul A. Wilson[4*]

1. Department of Earth Sciences, The University of Hong Kong, Hong Kong, China
2. State Key Laboratory of Loess and Quaternary Geology, Institute of Earth Environment, Chinese Academy of Sciences, Xi'an, China
3. School of Earth Sciences, Zhejiang University, Hangzhou, China
4. National Oceanography Centre Southampton, University of Southampton, Southampton, UK

* e-mail: zhliu@hku.hk (Z. L.) & paul.wilson@noc.soton.ac.uk (P. A. W.)

During the Late Paleogene between ~40 and 23 million years ago (Ma), Earth transitioned from a warm non-glaciated climate state and developed large dynamic ice sheets on Antarctica. This transition is largely inferred from the deep sea oxygen isotope ($\delta^{18}O$) record because records from independent temperature proxies are sparse. Here we present a 25-million-year-long alkenone-based record of surface temperature change from the North Atlantic Ocean. Our long temperature record documents peak warmth (~29 °C) during the Middle Eocene, a slow overall decline to the Eocene-Oligocene Transition (EOT, ~34 Ma), and high-amplitude variability (between ~28 and 24 °C) during the Oligo-Miocene. The overall structure of the record is similar to that of the deep sea $\delta^{18}O$ record, but a distinct anomaly is also evident. We find no evidence of surface cooling in the North Atlantic directly coinciding with the EOT when Antarctica first became cold enough to sustain large ice sheets and subantarctic waters cooled substantially. Surface ocean cooling during the EOT was therefore strongly asymmetric between hemispheres. This transient thermal decoupling of the North Atlantic Ocean from the southern high latitudes suggests that Antarctic glaciation triggered changes in ocean circulation-driven heat transport and influenced the far-field climate response.

During the Late Paleogene, Earth's climate transitioned from a warm largely unglaciated state with weak latitudinal temperature gradients to a world that was cold enough at high latitudes to sustain large ice sheets on Antarctica[1-4]. The pivotal event in this long-term transition to the modern glaciated climate state occurred across the Eocene-Oligocene Transition (EOT)[5, 6] between ~34 and 33 million years ago (Ma). The EOT is marked by substantial climatic and oceanic reorganization, including atmospheric CO_2 drawdown[7, 8], high-latitude cooling[9], widespread Antarctic glaciation, and deepening of the carbonate compensation depth[6] and northward migration of the Intertropical Convergence Zone[10] in the Pacific. It has also been suggested that the EOT marked the initiation of Atlantic Meridional Overturning Circulation (AMOC)[11-13], whereas the Antarctic Circumpolar Current[14] and modern ocean structure[15] are suggested to have developed later around 30 Ma. Once established, the early Antarctic ice sheets appear to have been extremely dynamic in response to orbitally paced changes in high latitude climate forcing[1, 4, 6].

The primary evidence for this increasingly well-established Late Paleogene environmental interpretation is the long-term overall increase in deep-sea benthic foraminiferal $\delta^{18}O$ values since the middle Eocene[1-4]. Yet, we know little about the way in which the surface oceans drove or responded to these changes. Data on contemporaneous change in surface ocean temperature for this interval are sparse[16] so trends are largely inferred from benthic $\delta^{18}O$ changes, which are controlled by both the continental ice sheet budget and deep sea temperature. Deconvolving the contribution of these two factors to changes in the $\delta^{18}O$ records has proven challenging and sometimes problematic[6, 9, 17]. Long temperature records using independent methods are needed from strategically positioned sites to address this problem and test competing hypotheses for the underlying forcing mechanisms responsible for the inferred Cenozoic transition to a glaciated climate state. The cause of the EOT is a subject of ongoing vigorous debate and two main hypotheses are now advanced: (i) the seminal hypothesis of gateway-driven Antarctic isolation[18] and (ii) a slow long-term decline in atmospheric CO_2 levels[19]. Ocean circulation change has been proposed as both a driving mechanism for Antarctic glaciation[20] and as a feedback process in response to glaciation[21]. However, these suggestions remain poorly tested because of the lack of datasets from the North Atlantic Ocean where there is a widespread upper Eocene- lower Oligocene unconformity at many deep-sea sites attributed to bottom current activity[22]. In fact, we lack detailed information for the Late Paleogene-Early Neogene time interval from all the mid- and high latitude regions of the Northern Hemisphere[9, 23, 24].

Here we report a 25-million-year-long record of surface ocean temperature spanning the Middle Eocene to Early Miocene (~43 to 18 Ma) from Integrated Ocean

Drilling Program (IODP) Site U1404 on the Newfoundland Margin in the mid-latitude northwest North Atlantic Ocean (40.00°N, 51.60°W; Fig. 1, 2). This site is located at the northern edge of the North Atlantic subtropical gyre and influenced by both the warm Gulf Stream and cold Deep Western Boundary Current (DWBC)[25]. Warm northward flowing surface waters meet the cold Labrador Current immediately to the north of the study site, resulting in a steep latitudinal surface ocean temperature gradient. Thus although Site U1404 is not situated within the modern day source region of North Atlantic Deep Water formation, it is situated just downstream and sensitive to AMOC changes[26, 27]. Modern mean annual surface ocean temperature at Site U1404 is 20°C (~19.5°C at its Oligocene paleo-location[28]; Methods, Fig. 1). Age control for our Site U1404 study section is based on biostratigraphic and magnetostratigraphic datums identified in shipboard analysis[25] (Supplementary Fig. 1, Table S1) together with a bulk carbonate $\delta^{18}O$ record spanning the EOT (Methods, Table S1), revealing a largely complete sequence spanning the middle Eocene to early Miocene. The alkenone unsaturation index ($U^{K'}_{37}$), a reliable temperature proxy successfully applied to sediments of similar age in previous studies[9, 29-31], is used to reconstruct surface ocean temperature changes at Site U1404 (Methods, Table S2). Alkenone concentration is also reported to infer surface productivity changes (Methods).

Site U1404 alkenone temperature & concentration trends

Because IODP Site U1404 was drilled into a sediment drift[25] located directly in the flow path of the modern day DWBC and Gulf Stream (Fig. 1), we must consider the influence (Methods) of lateral advection of suspended materials and sediment reworking on the temperature records that we reconstruct, especially for samples with low alkenone concentration. However, three lines of evidence suggest that these potential influences have not obscured the primary *in situ* environmental signal. First, alkenone-derived temperatures from both surface waters and modern sea-floor sediments in the region today do not show substantial deviations (within ±1.1°C) from measured surface ocean temperatures[32]. Second, our surface ocean temperature record is broadly consistent in structure with two low-resolution records[9] from sites further north (Fig. S2) and, together, these three mid-to-high latitude North Atlantic temperature records display a distinct latitudinal temperature gradient, essentially ruling out a major confounding contribution to Site U1404 from reworked old alkenones. Third, the EOT signal in our record (no cooling, Fig. 3) is inconsistent with that predicted by syn-sedimentary delivery of alkenones from further north by the DWBC carrying a cool temperature signal. We infer, therefore, that our record is representative of surface ocean temperature evolution in the mid-latitude North Atlantic Ocean during the Eocene to Miocene.

Alkenone concentrations at Site U1404 are typically lower than 10 ng/g in Middle and Late Eocene sediments, show marked fluctuations in sediments of earliest Oligocene age (~0–50 ng/g), and oscillate at relatively high levels in Oligo-Miocene sediments younger than ~31 Ma (~10–250 ng/g) (Fig. 2c). In some samples older than ~31 Ma, alkenone abundance was extremely low (Fig. 2c), yielding unreliable temperature estimates (Methods) that were excluded from our analysis (Fig. 2b). Overall, the long-term alkenone concentration signal is opposite in sign to the $U^{K'}_{37}$ temperature signal. The marked long-term increase in alkenone abundance across the EOT at Site U1404 (Fig. 2, S3) does not appear to be directly associated with surface temperature changes and may reflect surface ocean productivity in response to circulation changes[11-15, 21]. For most of the study period, short-term warming events are associated with modest transient increases in alkenone concentration (Fig. 2, S4), which are perhaps explained by nutrient advection in the subtropical gyre[33] (Methods).

Long-term Eocene to Oligocene surface temperature evolution

During the Late Paleogene, surface ocean temperatures at IODP Site U1404 varied between ~24 and at least 28°C, with maximum temperatures near the Middle Eocene Climatic Optimum (MECO; ~40 Ma)[30] and minimum temperatures in the Oligocene–earliest Miocene interval at ~32.5, ~26.5 and ~22.5 Ma (Fig. 2b). Largely consistent with the structure of the benthic $\delta^{18}O$ record[3] (Fig. 2a), surface ocean temperatures remained above 28°C around the time of MECO and cooled by roughly 1 to 2°C through the Late Eocene. The mid-Oligocene interval was characterized by marked surface ocean temperature fluctuations (up to ~4°C) that resemble the structure of the $\delta^{18}O$ record[1-4], with temperatures nearly reaching Late Eocene levels (~27–28°C) between ~31 and 29 Ma, followed by cooler temperatures (~24–26°C) between ~29 and 26 Ma during the Mid-Oligocene Glacial Interval, MOGI[1]. In the Late Oligocene, our record documents a warming trend which initiated at ~26 Ma and culminated around ~23.5 Ma, consistent with $\delta^{18}O$-based interpretations[1, 4]. The overall warmth of the latest Oligocene-Early Miocene is interrupted by transient cooling of between 2°C and 3°C across the Oligocene-Miocene Transition (Fig. 2b).

Throughout most of the Site U1404 study interval, surface ocean temperatures are warmer than 25°C. This finding demonstrates that the 25°C isotherm in the North Atlantic Ocean was positioned ~15° latitude (>1500 km) to the north of its modern position (Fig. 1) for most of the Late Paleogene. This result is likely attributable, at least in part, to a more expanded warm subtropical gyre system in the Paleogene relative to present day. Data from additional sites are needed to validate this interpretation, but the combination of warm temperatures (Fig. 2b) and very low alkenone abundances (Fig. 2c) seen in our records strongly suggests that Site U1404 was bathed by subtropical gyre waters during the Middle to Late Eocene.

Our data, together with existing records[9, 23, 24, 29-31, 34], reveal the broad picture of surface ocean temperature evolution during the Late Paleogene (Fig. S2), showing exceptional warmth in the Middle Eocene and a long-term cooling trend from the Middle Eocene to Early Oligocene. Our temperature record provides strong independent support for attributing the $\delta^{18}O$-inferred weak latitudinal temperature gradients in the surface ocean and warm deep ocean temperatures of the Eocene to an environmental control[35], not diagenetic aliasing[36].

In published data sets, surface ocean temperatures in the northern high-latitude and subantarctic regions cooled substantially from above 25°C around MECO to ~20°C just prior to the EOT (~34 Ma), and decreased further to 10 to 20°C in the Early to mid-Oligocene in both hemispheres (Fig. S2). Our data show that the amplitude of cooling off Newfoundland was modest in comparison (Fig. S2). Although not directly comparable, our alkenone-based temperature estimates also appear to be warmer than the modeled global air temperatures[37] and terrestrial temperatures from central North America[23], which decreased from ~18°C to ~16°C and from ~21°C to ~13°C respectively from the Late Eocene to Early Oligocene.

Thermal asymmetry across the EOT

Temperature changes during the EOT interval (34-33 Ma) show distinct northern–southern hemispheric asymmetry in the Atlantic. In the Southern Hemisphere, best expressed at subantarctic South Atlantic Site 511 (Fig. 3b, S2), surface ocean temperatures cooled by ~4 to 10°C, directly associated with the Earliest Oligocene Glacial Maximum (EOGM) at 33.6-33.2 Ma and sustained at least until ~32 Ma. However at Site U1404 in the North Atlantic there is little contemporaneous change associated with the EOGM (Fig. 3b), and Early Oligocene cooling occurs but not until at least 400 kyr after the main phase of Antarctic ice sheet growth (Fig. 3b). Overall, surface ocean temperatures at Site U1404 show a cooling trend from the EOGM to ~32 Ma, opposite to the recovery seen in benthic $\delta^{18}O$ and different from the trend at Site 511 (Fig. 3, S3). The fluctuating temperatures in this interval in the northern high latitudes, based on very limited data from Sites 336 and 913, seem to differ from those at subantarctic Site 511 where surface temperature remained low post-EOGM (Fig. 3), but more complete records are needed to assess whether the northern high latitudes followed the cooling trend documented at Site U1404.

In the Late Eocene, temperatures in the intervals 36.5-35 Ma and 34.5-34 Ma are undocumented because of low alkenone abundance (Fig. 2) but, based on the fine-scale association between alkenone concentration and temperature in our records (Fig. S4), are likely to have been relatively cool. Based on samples with trusted data, our record indicates a ~1-2°C cooling through the Late Eocene following the MECO and thus does not support the warming trend invoked[20] between ~37 and 34 Ma based on coccolith $\delta^{18}O$ in the equatorial Atlantic. The thermal asymmetry between sites U1404 and 511 is minimal during the Late Eocene in comparison to the earliest Oligocene (Fig. 3b). Increasing evidence[11-13] suggests that the 37-34 Ma interval is critical to understanding the early development of AMOC. Our incomplete record during this interval prevents us from confidently linking surface temperature changes to the detailed early history of AMOC. Yet, short-lived warming pulses around ~34.5 Ma and ~34 Ma identified here appear to coincide with the proposed timing of AMOC initiation based on diverse lines of evidence[11-13].

Our new temperature record from Site U1404 points to thermal decoupling of the northwest North Atlantic Ocean from the subantarctic South Atlantic Ocean across the EOT (Fig. 3). The general correspondence of the Site U1404 temperature trends to benthic $\delta^{18}O$ before the EOT and after ~31 Ma (Fig. 2) indicates that this thermal decoupling of the northwest Atlantic Ocean was transient, presumably reflecting surface temperature adjustments in the North Atlantic in response to ocean circulation and structure changes[14, 15, 21] and perhaps further development of AMOC as a primary control on climate[11-13]. The transient nature of this thermal decoupling is broadly consistent with terrestrial[38] vegetation and temperature changes. The distinct inter-hemispheric asymmetry in the surface ocean temperature change suggests that changes in ocean circulation and meridional heat transport were important across the EOT. In addition to the hypothesized impact of the subsidence of the Greenland-Scotland Ridge[12, 13], numerical simulations suggest that both Antarctic glaciation[21] and Southern Ocean gateway opening[11, 39] can bring about substantial ocean circulation changes, although the detailed results of these simulations are likely model dependent[11, 21, 39-41]. In terms of surface temperature response, Goldner *et al.*[21] simulated greater cooling in southern high latitudes than in the Northern Hemisphere in response to Antarctic glaciation, while Elsworth *et al.*[11] demonstrated a warming effect in the Northern Hemisphere and cooling in the Southern Hemisphere through Drake Passage deepening, both of which are mechanisms capable of inducing the hemispheric thermal asymmetry observed here. The transient nature and timing of the thermal asymmetry seems to favor a role for Antarctic glaciation, although the impact of slow long-term tectonic processes is difficult to assess here.

In summary, our record of Late Paleogene surface ocean temperatures from the Newfoundland Margin largely mimics the structure of benthic $\delta^{18}O$ change except during the EOT interval and reveals that the North Atlantic was very warm in comparison to today, even during the MOGI[1]. The Site U1404 alkenone temperature record substantiates an environmental explanation for the weak $\delta^{18}O$ latitudinal gradients in planktonic foraminiferal calcite records and provides direct evidence for inter-hemispheric differences in surface ocean temperature evolution across the EOT. This finding suggests that Antarctic glaciation triggered changes in ocean circulation that had a far-field influence on oceanic[21] and atmospheric[10] reorganization across the EOT.

Online Content Methods, including statements of data availability and any associated references, are available in the online version of the paper.

References

1. Liebrand, D. *et al*. Evolution of the early Antarctic ice ages. *Proc. Natl. Acad. Sci. USA* **114**, 3867-3872 (2017).
2. Zachos, J. C., Pagani, M., Sloan, L., Thomas, E. & Billups, K. Trends, rhythms, and aberrations in global climate 65 Ma to present. *Science* **292**, 686-693 (2001).
3. Cramer, B. S., Toggweiler, J. R., Wright, J. D., Katz, M. E. & Miller, K. G. Ocean overturning since the Late Cretaceous: Inferences from a new benthic foraminiferal isotope compilation. *Paleoceanography* **24**, PA4216 (2009).
4. Pälike, H. *et al*. The heartbeat of the Oligocene climate system. *Science* **314**,

1894-1898 (2006).

5. Miller, K. G., Wright, J. D. & Fairbanks, R. G. Unlocking the ice house: Oligocene–Miocene oxygen isotopes, eustasy, and margin erosion. *J. Geophys. Res.* **96**, 6829-6848 (1991).

6. Coxall, H. K., Wilson, P. A., Pälike, H., Lear, C. H. & Backman, J. Rapid stepwise onset of Antarctic glaciation and deeper calcite compensation in the Pacific Ocean. *Nature* **433**, 53-57 (2005).

7. Pearson, P. N., Foster, G. L. & Wade, B. S. Atmospheric carbon dioxide through the Eocene–Oligocene climate transition. *Nature* **461**, 1110-1113 (2009).

8. Pagani, M. *et al.* The role of carbon dioxide during the onset of Antarctic glaciation. *Science* **334**, 1261-1264 (2011).

9. Liu, Z. *et al.* Global cooling during the Eocene-Oligocene climate transition. *Science* **323**, 1187-1190 (2009).

10. Hyeong, K., Huroda, J., Seo, I. & Wilson, P. A. Response of the Pacific inter-tropical convergence zone to global cooling and initiation of Antarctic glaciation across the Eocene Oligocene Transition. *Sci. Rep.* **6**, 30647 (2016).

11. Elsworth, G., Galbraith, E. Halverson, G. & Yang, S. Enhanced weathering and

CO_2 drawdown caused by latest Eocene strengthening of the Atlantic meridional overturning circulation. *Nat. Geosci.* **10**, 213-216 (2017).

12. Abelson, M. & Erez, L. The onset of modern-like Atlantic meridional overturning circulation at the Eocene-Oligocene transition: Evidence, causes, and possible implications for global cooling. *Geochem. Geophys. Geosyst.* **18**, 2177-2199 (2017).

13. Coxall, H. K. *et al.* Export of nutrient rich Northern Component Water preceded early Oligocene Antarctic glaciation. *Nat. Geosci.* doi:10.1038/s41561-018-0069-9 (2018, in press).

14. Scher, H. D. *et al*. Onset of Antarctic Circumpolar Current 30 million years ago as Tasmanian Gateway aligned with westerlies. *Nature* **523**, 580-583 (2015).

15. Katz, M. E. *et al*. Impact of Antarctic circumpolar current development on Late Paleogene ocean structure. *Science* **332**, 1076-1079 (2011).

16. Norris, R. D. *et al.* Marine ecosystem responses to Cenozoic global change. *Science* **341**, 492-498 (2013).

17. Lear, C. H., Elderfield, H. & Wilson, P. A. Cenozoic deep-sea temperatures and global ice volumes from Mg/Ca in benthic foraminiferal calcite. *Science* **287**, 269-272 (2000).

18. Kennett, J. P. Cenozoic evolution of Antarctic glaciations, the circum-Antarctic ocean and their impact on global paleoceanography. *J. Geophys. Res.* **82**, 3843-3860 (1977).

19. DeConto, R. M. & Pollard, D. Rapid Cenozoic glaciation of Antarctica induced by declining atmospheric CO_2. *Nature* **421**, 245-249 (2003).

20. Tremblin, M., Hermoso, M. & Minoletti, F. Equatorial heat accumulation as a long-term trigger of permanent Antarctic ice sheets during the Cenozoic. *Proc. Natl. Acad. Sci. USA* **113**, 11782-11787 (2016).

21. Goldner, A., Herold, N. & Huber, M. Antarctic glaciation caused ocean circulation changes at the Eocene–Oligocene transition. *Nature* **511**, 574-577 (2014).

22. Miller, K. G. & Tucholke, B. E. in *Structure and Development of the Greenland-Scotland Ridge* (eds Bott, M. H. P., Saxov, S., Talwani, M. & Thiede, J.) 549-589 (Plenum, New York, 1983).

23. Zanazzi, A., Kohn, M. J., MacFadden, B. J. & Terry, D. O. Large temperature drop across the Eocene-Oligocene transition in central North America. *Nature* **445**, 639-642 (2007).

24. Schouten, S. *et al.* Onset of long-term cooling of Greenland near the Eocene-Oligocene boundary as revealed by branched tetraether lipids. *Geology* **36**,

147-150 (2008).

25. Norris, R. D., Wilson, P. A., Blum, P. & the Expedition 342 Scientists. In *Proc. Integrated Ocean Drilling Program* Vol. **342**, doi:10.2204/iodp.proc.342.105.2014 (Integrated Ocean Drilling Program, 2014).

26. Vellinga, M. & Wood, R. A. Impacts of thermohaline circulation shutdown in the twenty-first century. *Clim. Change* **91**, 43-63 (2008).

27. Stouffer, R. J. *et al*. Investigating the causes of the response of the thermohaline circulation to past and future climate changes. *J. Clim.* **19**, 1365-1387 (2006).

28. Matthews, K. J. *et al*. Global plate boundary evolution and kinematics since the late Paleozoic. *Global Planet. Change* **146**, 226-250 (2016).

29. Weller, P. & Stein, R. Paleogene biomarker records from the central Arctic Ocean (Integrated Ocean Drilling Program Expedition 302): organic carbon sources, anoxia, and sea surface temperature. *Paleoceanography* **23**, doi:10.1029/2007PA001472 (2008).

30. Bijl, P. K. *et al*. Transient middle Eocene atmospheric CO_2 and temperature variations. *Science* **330**, 819-821 (2010).

31. Plancq, J., Mattioli, E., Pittet, B., Simon, L. & Grossi, V. Productivity and sea-surface temperature changes recorded during the late Eocene-early Oligocene

at DSDP Site 511 (South Atlantic). *Palaeogeogr. Palaeoclimatol. Palaeoecol.* **407**, 34-44 (2014).

32. Conte, M. H. *et al.*, Global temperature calibration of the alkenone unsaturation index ($U^{K'}_{37}$) in surface waters and comparison with surface sediments. *Geochem. Geophys. Geosyst.* **7**, Q02005 (2006).

33. Palter, J. B., Lozier, M. S. & Barber, R. T. The effect of advection on the nutrient reservoir in the North Atlantic subtropical gyre. *Nature* **437**, 687-692 (2005).

34. Bijl, P. K. *et al.* Early Palaeogene temperature evolution of the southwest Pacific Ocean. *Nature* **461**, 776-779 (2009).

35. Zachos, J. C., Stott, L. D. & Lohmann, K. C. Evolution of early Cenozoic marine temperatures. *Paleoceanography* **9**, 353-387 (1994).

36. Bernard, S., Daval, D., Ackerer, P., Pont, S. & Meibom, A. Burial-induced oxygen-isotope re-equilibration of fossil foraminifera explains ocean paleotemperature paradoxes. *Nat. Commun.* **8**, 1134 (2017).

37. Stap, L. B., van de Wal, R. S. W., de Boer, B., Bintanja, R. & Lourens, L. The influence of ice sheets on temperature during the past 38 million years inferred from a one-dimensional ice sheet-climate model. *Clim. Past* **13**, 1243-1257 (2017).

38. Pound, M. J. & Salzmann, U. Heterogeneity in global vegetation and terrestrial climate change during the late Eocene to early Oligocene transition. *Sci. Rep.* **7**, 43386 (2017).

39. Yang, S., Galbraith, E. & Palter, J. Coupled climate impacts of the Drake Passage and the Panama Seaway. *Clim. Dyn.* **43**, 37-52 (2014).

40. Ladant, J.-B., Donnadieu, Y., Bopp, L., Lear, C. H. & Wilson, P. A. Meridional contrasts in productivity changes driven by the opening of Drake Passage. *Paleoceanography and Paleoclimatology* **33**, 302-317 (2018).

41. Hutchinson, D. K. *et al*. Climate sensitivity and meridional overturning circulation in the late Eocene using GFDL CM2.1. *Clim. Past,* https://www.clim-past-discuss.net/cp-2017-161/ (2018)

Acknowledgments

We dedicate this contribution to Mark Pagani. This research used samples provided by the Integrated Ocean Drilling Program (IODP), which is sponsored by the US National Science Foundation and participating countries under management of Joint Oceano- graphic Institutions, Inc. We thank the scientists, technicians and support staff of IODP Expedition 342, IODP China and IODP UK for support. This research was supported by National Key Research and Development Program of China

(2016YFE0109500), Chinese Academy of Sciences (QYZDY-SSW-DQC001, ZDBS-SSW-DQC001) (to W.L & Z.L.), Hong Kong Research Grant Council Grant 17303614 (to Z.L.), UK Natural Environment Research Council (NERC) Grant NE/L007452/1 (to S.M.B), NERC Grant NE/K014137/1 (to P.A.W.) and a Royal Society Wolfson award (to P.A.W.). We thank Helen Coxall and two anonymous referees for their very thorough and constructive reviews.

Author Contributions P.A.W. and Z.L. participated in IODP Expedition 342 in seagoing capacities. Z.L., S.M.B and P.A.W. conceived the idea of generating a late Paleogene temperature record. Y.H. and Y.J. performed alkenone analysis while H.W. and W.L. completed carbonate oxygen isotope work. Z.L. and P.A.W. led the writing of the manuscript with intellectual contributions from all co-authors.

Additional Information

Supplementary Information is available in the online version of paper.

Reprints and permissions information is available at www.nature.com/reprints.

The authors declare no competing **financial interests**.

Correspondence and requests for materials should be addressed to Z.L. (zhliu@hku.hk) and P.A.W. (paul.wilson@noc.soton.ac.uk).

Figure captions

Figure 1 | Modern and paleo locations of IODP Site U1404, superimposed on modern mean annual surface temperature field in the North Atlantic. Map template made with Ocean Data View. The tectonic backtracks of U1404 are indicated in 0.5 Myr steps (Methods) and highlighted at 43 Ma, EOT (Eocene-Oligocene Transition) age, and 18 Ma. Inset map indicates sites of surface temperature records used or cited, from refs 9, 23 (Central North America), 24, 29-31, and this study. DWBC, Deep Western Boundary Current; GS, Gulf Stream; NAC, North Atlantic Current; LSC, Labrador Sea Current.

Figure 2 | Late Paleogene records of alkenone temperature and content from Site U1404. **a**, global benthic $\delta^{18}O$ record[3], with "ice-free" temperature scale for the Eocene[2]. **b**, surface ocean temperature. **c**, alkenone content. Concentration <2.5 ng/g (dashed line) but trusted temperature measurements achieved (Methods) indicated with light-green filled circles in **c**, and their temperatures as empty orange circles in **b**. Data points before 31 Ma disconnected in **b**, **c** due to unreported temperatures from low alkenone contents (empty circles in **c**). Warm intervals highlighted with light-yellow bars. MECO, Middle Eocene Climatic Optimum; MOGI, Mid-Oligocene Glacial Intervals; OMT, Oligocene-Miocene Transition.

Figure 3 | Detailed view of $\delta^{18}O$ and relative surface ocean temperature changes across the EOT. a, bulk carbonate $\delta^{18}O$ from Site U1404, with analytical uncertainty indicated by error bars, superimposed on the global benthic $\delta^{18}O$ record[3]. **b**, relative temperature changes. The two dashed lines in **b** indicate different trends from ~33.6 Ma**.** Temperature changes (ΔTemp.) are relative to mean values at 37-34 Ma at their respective sites. Note different scales used for temperature changes at U1404 versus other sites (see Fig. S2 for U404 data plotted on the same scale as other sites).

Methods

Materials and chronology. Samples were collected from IODP Site U1404 (40.00°N, 51.60°W, water depth 4742 m) during IODP Expedition 342 (ref 25, Fig. 1). The sedimentary sequence at this site mainly cover the interval from the Middle Eocene to Early Miocene at Site U1404 (ref 42). We analyzed ~360 sediment samples (~20 cm^3, 10-30 gram dry weight) from Site U1404 Holes A and B. Sample spacing was adjusted according to changes in average sedimentation rate. Overall, the temporal resolution of our record is ~1 sample per 60-80 kyr.

Age control points are taken from shipboard planktonic foraminifers, radiolarians, calcareous nannofossils, and paleomagnetics, which yield average linear sedimentation rates varying from 0.27 cm/kyr during the Late Eocene-Early Oligocene to 8.0 cm/kyr in the Early Miocene[42]. The Bayesian program Bacon[43] was used to fit the age-depth profile at Site U1404 to derive the final chronology (Fig. S1). As our sampling plan followed a slightly updated, but not formally published, core composite depth below sea floor (CCSF-m) that was circulated within the Expedition 342 sampling party, we use this updated version over the published CCSF-m scheme[42]. Based on the results generated here and the datums identified in both holes, the updated CCSF-m yields an improved ‘splice’ of Holes A and B. In supplementary files (Table S1, S2), we provide CSF-m, published and updated CCSF-m for all the datums used and samples analyzed here.

The Site U1404 chronology is generally well controlled in most sections. More uncertainty exists in the Middle Oligocene section, where two datums, *Bc Triquetrorhabdulus carinatus* and *B Sphenolithus ciperoensis* (Table S1), ~3-Myr apart, were identified within 1 m (222.67-223.36 CCSF-m) (Fig. S1). We estimate that in extreme cases this would result in chronological uncertainty of ~2.4 Myr (Fig. S2). We used the $\delta^{18}O$ stratigraphy as an independent check, without using it to construct the U1404 chronology. This independent $\delta^{18}O$ stratigraphy confirms the presence of a condensed EOT interval (Fig. 3a). All ages are updated to the Gradstein (2012) timescale[44], including the composite benthic $\delta^{18}O$ record[3] to aid comparison.

Alkenone analysis. Sediments were freeze-dried, ground, and extracted with a Dionex Accelerated Solvent Extractor (ASE300). We performed basic hydrolysis on the extracted lipids and then separated them into 3 compound classes using silica column chromatography. The alkenone fraction was analyzed on an Agilent 7890 gas chromatograph (GC) with an Agilent J&W column (DB-1, 60 m x 0.25 mm i.d. x 0.1 µm film thickness) and H_2 (1.5 ml/min) as the carrier gas. The oven temperature was programed: 60°C (1 min) to 270°C at 20°C/min and then to 310°C (held 40 min) at 5°C/min. n-C_{36} alkane was used as external standard for alkenone quantifications. Analytical precision (1σ) for our laboratory standards is 0.005 unit (equivalent to 0.1-0.2°C) for the alkenone unsaturation index, $U^{K'}_{37}$ (ref 45), and 5% for alkenone content.

Alkenone content at this site is generally low in sediments older than ~31 Ma and much higher in younger ones (Fig. 2c). We rejected ~80 samples, ~22% of the total, due to low content or unidentifiable alkenones. We used the criterion that the amount of C_{37} alkenones injected into the GC has to be >10 ng to avoid the effect of preferential absorption of the $C_{37:3}$ alkenone on GC column[46]. We concentrated low content samples into 10-20 microliter (µl) volume and injected 2 µl into the GC. With, on average, ~20 g sediment, we estimated a cut-off concentration at ~2.5 ng/g (2.5 ng/g x 20 g /10 µl x 2 µl = 10 ng). For those samples falling just below <2.5 ng/g, we further concentrated the solution into <10 μl and reanalyzed them by GC. If the injected C_{37} amount reached 10 ng, temperature estimates from these samples (total ~30) were reported with those contents >2.5 ng/g (Fig. 2b). For those rejected samples with extremely low alkenone abundance (<2.5 ng/g), their calculated $U^{K'}_{37}$ values are abnormally low.

Alkenone surface ocean temperature assessment. Alkenones are organic compounds that are produced by a few species of haptophyte algae living in surface ocean waters[47], faithfully recording surface conditions. Alkenone content thus indicates surface haptophyte productivity and could further reflect the overall surface biological productivity[48]. The global core top-temperature equation[49], calibrated to mean annual surface temperatures, was used to convert the $U^{K'}_{37}$ index into temperature estimates. The lowest temperature estimate (~24°C) in our record is only warmer than the modern annual mean surface temperature (20°C, Fig. 1) by 4°C suggesting that our temperature estimates likely represent annual mean surface temperatures at the time. Maximum $U^{K'}_{37}$ values in our record are 0.98-0.99 (28.4-28.7°C), having not reached unity (29.0°C) and thus are still capable recording temperature changes, but perhaps represent conservative temperature estimates.

Our surface temperature reconstruction around and prior to the EOT is affected by the generally low alkenone content at U1404, a common problem for other localities[9]. Counterintuitively, extremely low alkenone abundances characterize relatively cool intervals before ~31 Ma (Fig. 2). Based on modern observations, Palter *et al.*[33] suggest that, under relatively cool conditions, enhanced winter-time upstream deep convective mixing and shallow subtropical mode water formation at the northern edge of the subtropical gyre reduce downstream nutrient availability and thus primary productivity within the gyre. This interpretation may explain the relationship between temperature and alkenone content observed here during short-lived events (Fig. 2, S4), especially if the subtropical gyre was expanded relative to today during the Late Paleogene with its northern limb poleward of our study site (Fig. 1). Thus, some cooler intervals before ~31 Ma are underrepresented in our record. However, no samples were rejected from the earliest Oligocene glacial maximum (Fig. 2c).

Potentially, temperature estimates from low-content samples are susceptible to the influence of lateral transport of reworked sediments or suspended materials. Deep water overflow from the Norwegian-Greenland Sea into the North Atlantic initiated probably during the Middle Eocene, associated with global cooling[50], or during the Late Eocene[12, 13]. However, subsidence of the Greenland-Scotland Ridge took place during the Early Oligocene[51], largely limiting the transport of reworked Arctic alkenones (surface temperature range of 10-25°C during the Middle Eocene[29]). Regardless, the generally warm temperatures at Site U1404 would suggest limited contribution from the Arctic. Temperatures in the high-latitude North Atlantic were generally above 20°C before the EOT[9] (Fig. S2), which should have little impact on the temperature estimates at our study site, if reworked alkenones were transported from the region. Possibly the lateral advection by the warm Gulf Stream or its prototype could also partially offset the cool signal from the north.

Carbonate $\delta^{18}O$ analysis. Isotope analysis followed the procedure in ref 52. Briefly, ~1 g sediment samples were ground in an agate mortar and sieved through a 100-mesh (150-µm) screen. Analyses of carbonate samples were performed using an isotope ratio mass spectrometer [MAT-252 (Finnigan)] with an automated carbonate preparation device (Kiel II) at the Institute of Earth Environment, Chinese Academy of Sciences. Oxygen isotope composition is expressed in the delta (δ) notation relative to the V-PDB standard. Repeated analyses of laboratory carbonate standards (TTB1, China national standard) with known $\delta^{18}O$ values were performed daily to ensure instrumental accuracy. The long-term instrument stability is monitored by the international NBS18 and NBS19 standards. Typical precision for the repeated analyses is smaller than ±0.1‰.

We analyzed ~60 carbonate samples from the rare carbonate-bearing sediments of EOT age at Site U1404. The bulk carbonate $\delta^{18}O$ changes at U1404, based on the shipboard chronology, coincide with the changes in the composite benthic $\delta^{18}O$ (Fig.

3a), thus confirming the derived chronology and the presence of the EOT section. As no carbonate is present between 34.1 and 33.8 Ma, our bulk $\delta^{18}O$ only records the major (second) step of $\delta^{18}O$ increase across the EOT[6], but the fit to the benthic $\delta^{18}O$ composite is remarkable (Fig. 3a) Thus, the hemispheric difference in surface temperature evolution at the time is unlikely to arise from chronological uncertainty.

Site backtracking. We calculated paleolatitude and paleolongtitude of the site in 0.5 Myr step using the GPlates software package (http://www.gplates.org/). Coastline and rotations were taken from refs 53 and 28 respectively. The modern annual mean surface temperature field is taken from the World Ocean Atlas[54], generated with Ocean Data View[55]. As the site moved little latitudinally over the studied period, no latitudinal correction on temperature changes was applied in this study.

Data availability. We declare that lists of the sources of previously published data supporting the findings of this study are available within the article and in the supplementary files. The new data are available in the supplementary files and will be archived at https://www.pangaea.de/.

References

42. Norris, R. D. *et al*. Site U1404. In *Proc. Integrated Ocean Drilling Program* Vol. **342** (eds Norris, R. D., Wilson, P. A., Blum, P. & the Expedition 342 Scientists), doi:10.2204/iodp.proc.342.105.2014 (Integrated Ocean Drilling Program, 2014).

43. Blaauw, M. & Christen, J. A. Flexible paleoclimate age-depth models using an autoregressive gamma process. *Bayesian Anal.* **6**, 457-474 (2011).

44. Gradstein, F. M., Ogg, J. G. & Schmitz, M. *The Geologic Time Scale 2012 2-Volume Set* (Elsevier, 2012).

45. Prahl, F. G., Muehlhausen, L. A. & Zahnle, D. L. Further evaluation of long-chain alkenones as indicators of paleoceanographic conditions. *Geochim. Cosmochim. Acta* **52**, 2303-2310 (1988).

46. Villanueva, J. & Grimalt, J. O. Gas chromatographic tuning of the $U^{K'}_{37}$ paleothermometer. *Anal. Chem.* **69**, 3329- 3332 (1997).

47. Brassell, S. C. Eglinton, G., Marlowe, I. T., Pflaumann, U. & Sarnthein, M. Molecular stratigraphy: A new tool for climatic assessment. *Nature* **320**, 129-133 (1986).

48. Lawrence, K. T., Liu, Z. & Herbert, T. D. Evolution of the eastern tropical Pacific through Plio-Pleistocene glaciation. *Science* **312**, 79-83 (2006).

49. Müller, P. J., Kirst, G., Rohland, G., von Storch, I. & Rosell-Melé, A. Calibration of the alkenone paleotemperature index $U^{K'}_{37}$ based on core-tops from the eastern South Atlantic and the global ocean (60°N-60°S). *Geochim. Cosmochim. Acta* **62**, 1757-1772 (1998).

50. Hohbein, M. W., Sexton, P. F. & Cartwright, J. A. Onset of North Atlantic Deep Water production coincident with inception of the Cenozoic global cooling trend. *Geology* **40**, 255-258 (2012).

51. Abelson, M., Agnon, A. & Almogi-Labin, A. Indications for control of the Iceland plume on the Eocene-Oligocene "greenhouse-icehouse" climate transition. *Earth Planet. Sci. Lett.* **265**, 33-48 (2008).

52. Liu, W. *et al*. Late Miocene episodic lakes in the arid Tarim Basin, western China. *Proc. Natl. Acad. Sci. USA* **111**, 16292-16296 (2014).

53. Seton, M. *et al*. Global continental and ocean basin reconstructions since 200 Ma. *Earth Sci. Rev.* **113**, 212-270 (2012).

54. Locarnini, R. A. *et al*. World Ocean Atlas 2013, Volume 1: Temperature. In *NOAA Atlas NESDIS 73* (Levitus, S. ed., Mishonov, A. technical ed.), 40 pp (Silver Spring, MD, 2013).

55. Schlitzer, R. Data Analysis and Visualization with Ocean Data View. *CMOS*

Bulletin SCMO **43**, 9-13 (2015).

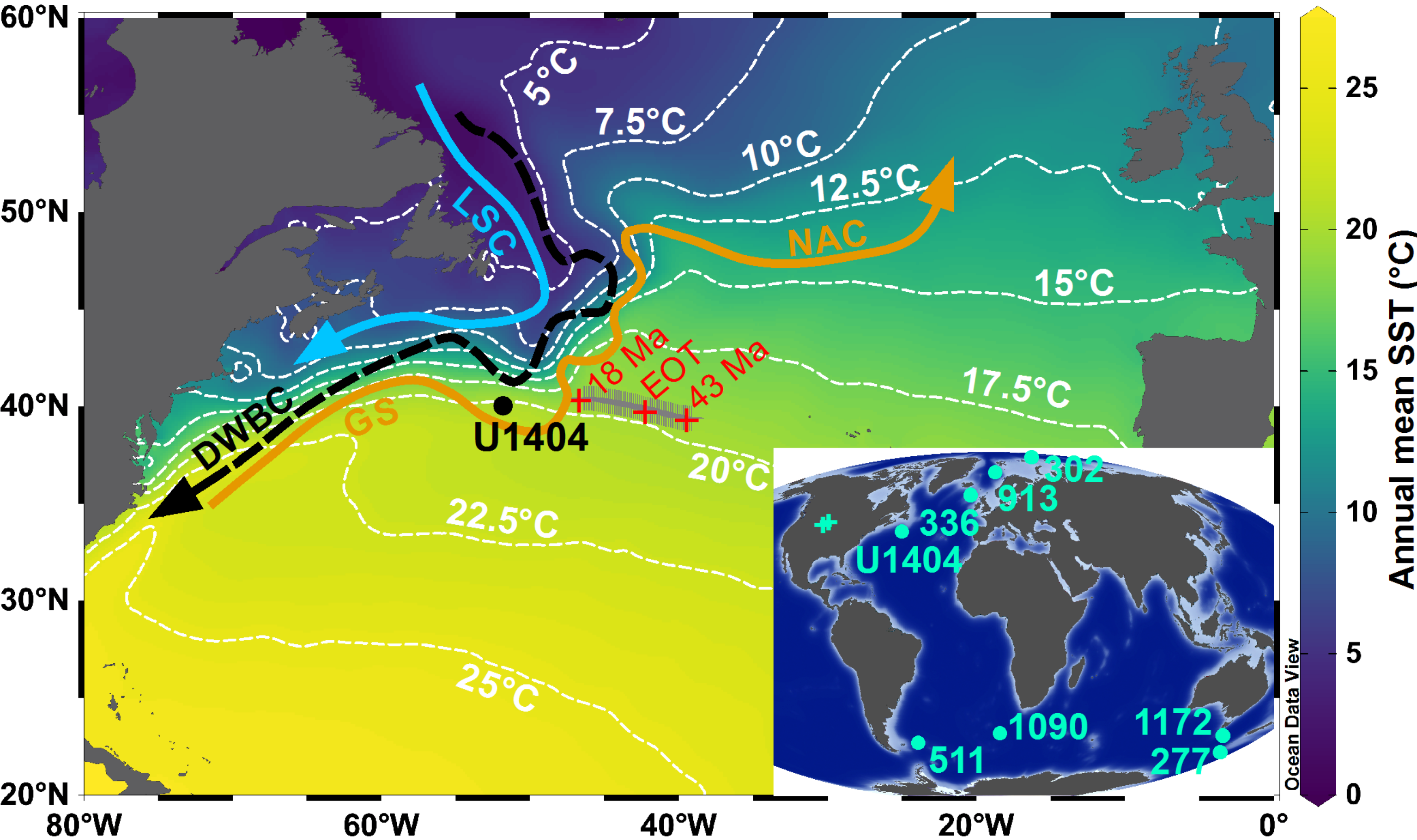
60°N
50°N
40°N
30°N
20°N
80°W
60°W
40°W
20°W
0°
5°C
7.5°C
10°C
12.5°C
15°C
17.5°C
20°C
22.5°C
25°C
LSC
NAC
GS
DWBC
U1404
18 Ma
EOT
43 Ma
302
913
336
U1404
1090
511
1172
277
Ocean Data View
Annual mean SST (°C)
0
5
10
15
20
25

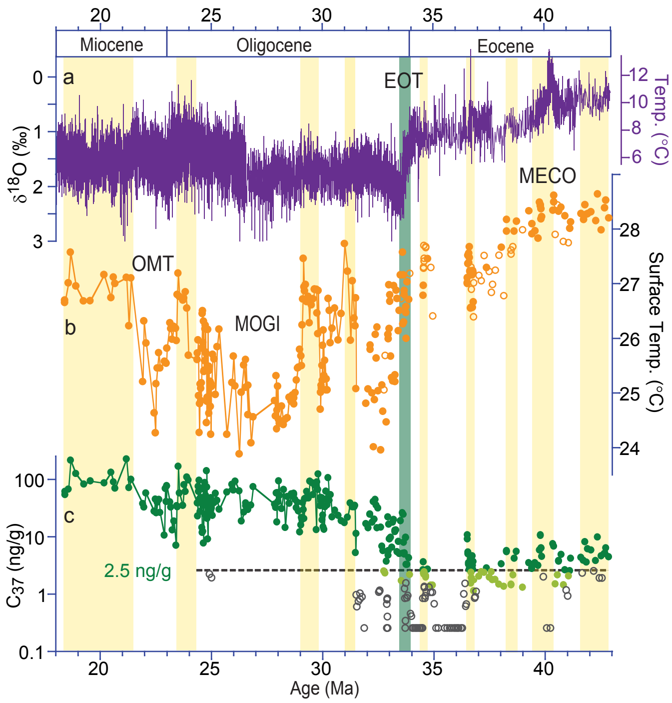

20
25
30
35
40
Miocene
Oligocene
Eocene
a
EOT
MECO
OMT
MOGI
b
c
δ18O (‰)
Temp. (°C)
Surface Temp. (°C)
C37 (ng/g)
2.5 ng/g
Age (Ma)

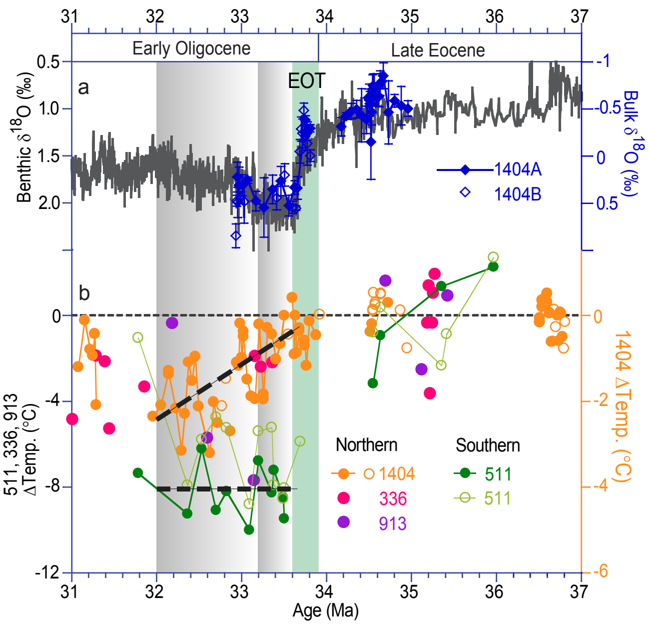

Early Oligocene
Late Eocene
EOT
a
b
Benthic δ18O (‰)
Bulk δ18O (‰)
1404A
1404B
511, 336, 913 ΔTemp. (°C)
1404 ΔTemp. (°C)
Northern
Southern
1404
336
913
511
511
Age (Ma)